PNAS RESEARCH ARTICLE | IMMUNOLOGY AND INFLAMMATION OPEN ACCESS

Targeting orthotopic and metastatic pancreatic cancer with allogeneic stem cell–engineered mesothelin-redirected CAR-NKT cells

Yan-Ruide Li[a,b], Xinyuan Shen[a,b], Enbo Zhu[a,b], Zhe Li[a,b], Jie Huang[a,b], Thuc Le[c,d], Catrina Tran[c,d], Caius G. Radu[c,e], and Lili Yang[a,b,e,f,g,h,i,1]

Affiliations are included on p. 11.

Edited by Carl June, University of Pennsylvania, Philadelphia, PA; received July 4, 2025; accepted October 13, 2025

Pancreatic cancer (PC) remains one of the leading causes of cancer-related mortality worldwide. The majority of patients are diagnosed at advanced stages, with over 50% presenting with metastatic disease at the time of diagnosis. Although chimeric antigen receptor (CAR)-T cell therapy has shown promise in targeting PC, its clinical efficacy remains limited due to several critical challenges. These include tumor antigen heterogeneity, antigen loss or escape mechanisms, functional exhaustion of CAR-T cells within the tumor microenvironment, as well as inherent limitations of autologous approaches such as high manufacturing costs, prolonged production timelines, and restricted scalability. To address these challenges, we developed allogeneic IL-15–enhanced, mesothelin-specific CAR-engineered invariant natural killer T (^{Allo15}MCAR-NKT) cells through gene engineering of human hematopoietic stem and progenitor cells (HSPCs) using a clinically guided culture method. These ^{Allo15}MCAR-NKT cells exhibited robust and multifaceted antitumor activity against PC, driven by both CAR and NK receptor–mediated cytotoxic mechanisms. In orthotopic and metastatic human PC xenograft models, ^{Allo15}MCAR-NKT cells demonstrated superior tumor control, enhanced trafficking and infiltration into tumor sites, sustained effector and cytotoxic phenotypes, and reduced expression of exhaustion markers. Importantly, ^{Allo15}MCAR-NKT cells demonstrated a favorable safety profile, characterized by the absence of graft-versus-host disease and minimal cytokine release syndrome. Collectively, these findings validate ^{Allo15}MCAR-NKT cells as a promising next-generation, off-the-shelf immunotherapeutic approach for PC, with the potential to overcome critical challenges including tumor heterogeneity, immune evasion, and therapeutic resistance, especially in the context of metastatic disease.

Pancreatic cancer (PC) | invariant natural killer T (NKT) cell | chimeric antigen receptor (CAR) | allogeneic cell therapy | metastatic cancer

Significance

Pancreatic cancer (PC) is one of the deadliest cancers, often diagnosed at advanced, hard-to-treat stages. Current cell-based therapies like CAR-T cells face major hurdles, including tumor variability, immune escape, and limited scalability. In this study, we developed an off-the-shelf immunotherapy using gene-engineered natural killer T cells derived from stem cells—called ^{Allo15}MCAR-NKT cells. These cells target pancreatic tumors through multiple killing mechanisms, resist immune exhaustion, and avoid rejection by the patient's immune system. In preclinical models, they effectively controlled tumor growth and spread. This work offers a promising step toward scalable, next-generation immunotherapy for PC, with the potential to address current treatment limitations and improve outcomes for patients with advanced disease.

Pancreatic cancer (PC) is a leading cause of cancer-related death worldwide with a 5-y survival rate below 12% (1). Most patients are diagnosed at an advanced stage, and over 50% present with metastatic disease at diagnosis (2). Median survival for metastatic cases is under one year—often around four months—with 5-y survival rates as low as 2 to 3% despite aggressive chemotherapy (3). Common metastatic sites include the liver, peritoneum, and lungs, contributing to rapid clinical deterioration and poor therapeutic response. Metastatic PC is largely refractory to chemotherapy and immune checkpoint inhibitors, in part due to a dense stromal barrier and an immunosuppressive tumor microenvironment (TME) (3). These features highlight the urgent need for new, scalable immunotherapies capable of targeting disseminated disease.

Chimeric antigen receptor (CAR)-engineered T (CAR-T) cell therapies have achieved major success in hematologic malignancies but face substantial barriers in solid tumors like PC, including poor tumor trafficking, TME-mediated immune suppression, and on-target off-tumor toxicity (4, 5). Mesothelin (MSLN) is a validated CAR target in PC, with high tumor expression and limited presence in normal tissues (6, 7). Early-phase clinical trials of MSLN-redirected CAR-T cell therapies have shown encouraging safety profiles and signs of antitumor activity (8, 9). However, their overall clinical efficacy has been limited by several challenges, including tumor antigen heterogeneity, antigen escape, and CAR-T cell dysfunction within the immunosuppressive TME. Moreover, the autologous nature of these therapies imposes significant constraints on scalability and accessibility due to the complexity, cost, and time required for individualized manufacturing (8, 9).

Invariant natural killer T (NKT) cells are a rare, innate-like T cell subset that recognize glycolipid antigens presented by the nonpolymorphic MHC class I-like molecule

Author contributions: Y.-R.L. and L.Y. designed research; Y.-R.L., X.S., E.Z., Z.L., J.H., T.L., C.T., and C.G.R. performed research; Y.-R.L. and L.Y. contributed new reagents/analytic tools; Y.-R.L. analyzed data; and Y.-R.L. wrote the paper.

Competing interest statement: L.Y. is a scientific advisor to AlzChem and Amberstone Biosciences, and a co-founder, stockholder, and advisory board member of Appia Bio. None of the declared companies contributed to or directed any of the research reported in this article. The remaining authors declare no competing interests.

This article is a PNAS Direct Submission.

[1]To whom correspondence may be addressed. Email: liliyang@ucla.edu.

This article contains supporting information online at https://www.pnas.org/lookup/suppl/doi:10.1073/pnas.2517786122/-/DCSupplemental.

Published November 21, 2025.

CD1d (10, 11). This unique restriction renders them incapable of initiating graft-versus-host disease (GvHD), enabling their safe use in allogeneic adoptive cell therapies (12–15). NKT cells bridge innate and adaptive immunity, rapidly producing cytokines and engaging in cytotoxic activity upon activation. When engineered with CARs, CAR-NKT cells combine tumor specificity with intrinsic TCR- and NK receptor (NKR)-mediated cytotoxicity, allowing them to target both tumor cells and suppressive myeloid populations within the immunosuppressive TME (16, 17). Compared to conventional CAR-T cells, CAR-NKT cells exhibit enhanced trafficking to solid tumors, driven by favorable chemokine receptor profiles (e.g., CXCR3 and CCR5), and demonstrate superior resistance to exhaustion and terminal differentiation (18–20). They are less prone to systemic cytokine release and neurotoxicity, and do not require HLA matching, broadening their clinical applicability across diverse patient populations (21–23). These attributes make CAR-NKT cells an attractive platform for developing off-the-shelf immunotherapies for solid tumors. However, the extremely low frequency of NKT cells in peripheral blood, typically comprising only 0.001% to 0.1% of circulating T cells in humans, poses a significant challenge for generating sufficient quantities for clinical application (10, 11). Thus, the development of robust strategies to produce CAR-NKT cells at high yield and purity is critical for advancing their therapeutic use.

Here, we report the development of allogeneic IL-15–enhanced, MSLN-redirected CAR-NKT (^{Allo15}MCAR-NKT) cells derived from gene-engineered human cord blood (CB) CD34$^+$ hematopoietic stem and progenitor cells (HSPCs) using a clinically guided, feeder-free differentiation protocol (24). We comprehensively evaluate the manufacturing process, phenotypic and functional characteristics, antitumor efficacy, mechanisms of action, biodistribution, safety, and immunogenicity of ^{Allo15}MCAR-NKT cells. Furthermore, we assessed their unique tumor-homing and infiltration capabilities using multiple human PC orthotopic and metastatic xenograft models. Together, these findings establish a strong preclinical foundation for the translational and clinical development of ^{Allo15}MCAR-NKT cells as an off-the-shelf immunotherapy for both primary and metastatic PC.

Results

Stem Cell–Derived Allogeneic IL-15-Enhanced MCAR-Engineered NKT (^{Allo15}MCAR-NKT) Cells Can be Generated Using a Clinically Guided Culture Method. We employed a previously established feeder-free differentiation platform to generate ^{Allo15}MCAR-NKT cells from human CB–derived CD34$^+$ HSPCs (20, 24). This platform was originally developed for the production of allogeneic CAR-NKT cells targeting hematologic malignancies such as BCMA-expressing multiple myeloma (MM) and CD33$^+$ acute myeloid leukemia (AML) (20, 24). In the present study, we adapted this strategy to develop CAR-NKT cells targeting solid tumors, with a specific focus on MSLN-positive PC (Fig. 1*A*).

To generate ^{Allo15}MCAR-NKT cells, CD34$^+$ HSPCs were transduced with a single lentiviral vector, Lenti/iNKT-MCAR-IL-15, encoding three essential components: 1) The invariant NKT TCR α and β chains, cloned from healthy donor PBMC-derived NKT cells, which have been validated for both autologous and allogeneic CAR-NKT cell generation (23, 25); 2) A third-generation, MSLN-targeting CAR based on the clinically established SS1 single-chain variable fragment (scFv), incorporating CD28 and 4-1BB costimulatory domains (26); and 3) A gene encoding human soluble IL-15, which enhances the proliferation, persistence, and antitumor activity of CAR-NKT cells derived from both PBMCs and HSPCs (*SI Appendix*, Fig. S1*A*) (18–20, 24). While we employed a third-generation CAR design due to some reports suggesting enhanced CAR-T cell expansion after infusion in humans (*SI Appendix*, Fig. S1*A*) (27), determining the optimal CAR configuration for allogeneic CAR-NKT therapy remains an important direction for future investigation. The transduction efficiency on CD34$^+$ HSPCs was high, with over 50% of cells expressing the integrated construct (Fig. 1*B*). Notably, the single-vector design ensures that each transduced HSPC expresses all three transgenes, eliminating the need for additional enrichment or selection steps (Fig. 1*A*).

Following transduction, engineered HSPCs were subjected to the six-week ex vivo differentiation culture: stage 1 HSPC expansion (2 wk), stage 2 NKT differentiation (1 wk), stage 3 NKT deep differentiation (1 wk), and stage 4 NKT expansion (2 wk) (28). The entire differentiation process was conducted under feeder-free and serum-free conditions to ensure clinical translatability (24). During stage 4 NKT expansion, K562-based artificial antigen-presenting cells (aAPCs) overexpressing MSLN were utilized to stimulate NKT cells, as these human feeder cells have been previously validated for clinical development (29). During the culture, cells progressively acquired the NKT lineage phenotype—reaching ~30% NKT cells at week 2, ~80% by week 4, and exceeding 97% by week 6 (Fig. 1*C*). The differentiation trajectory followed a typical T-lineage progression, transitioning from double-negative (DN; CD4$^-$CD8$^-$) to double-positive (DP; CD4$^+$CD8$^+$) stages, and ultimately maturing into either CD8$^+$ single-positive (SP) or DN NKT subsets (Fig. 1*C*) (11, 12, 30). The CD8$^+$ SP and DN populations are of particular interest due to its superior effector function and cytolytic capacity, making it especially suitable for solid tumor immunotherapy (10, 11, 31, 32).

By the end of culture, the ^{Allo15}MCAR-NKT cell product demonstrated high purity (>97%), with nearly all cells coexpressing the invariant NKT TCR and the MSLN-specific CAR (Fig. 1 *D* and *E*). This high level of transgene expression is attributable to positive selection during HSPC differentiation, ensuring that all final cells carry the transduced constructs (33, 34). Vector copy number (VCN) analysis of the ^{Allo15}MCAR-NKT cell product revealed an average of 3 to 4 copies per cell, corresponding to approximately 50 to 60% of cells positive for intracellular iNKT TCR staining at the HSPC engineering stage (Fig. 2*B* and *SI Appendix*, Fig. S1*B*). The resulting VCN per cell remained within clinically acceptable limits for CAR cell therapy (typically <5 copies per genome), supporting the safety of the product and indicating a minimal risk of insertional mutagenesis (35, 36). This robust manufacturing protocol also enabled substantial expansion: a single CB donor, yielding approximately 5×10^6 CD34$^+$ HSPCs, produced over 10^{12} ^{Allo15}MCAR-NKT cells, which are sufficient for producing an estimated 1,000 to 10,000 therapeutic doses (Fig. 1*F*). Importantly, this approach has proven consistent and reproducible across multiple CB donors, with stable yield and quality (Fig. 1 *E* and *F*).

In summary, this study demonstrates the successful adaptation of HSPC gene engineering for the production of MSLN-targeting ^{Allo15}MCAR-NKT cells. The use of a clinically scalable, feeder-free differentiation system resulted in a highly pure and potent cell product with strong potential for off-the-shelf application in solid tumor immunotherapy, including treatment of PC.

^{Allo15}MCAR-NKT Cells Display a Hybrid T/NK Cell Phenotype and Exhibit Strong Effector Functions and Cytotoxic Properties. We first characterized the phenotype and functional profile of ^{Allo15}MCAR-NKT cells and compared them with two benchmark groups: 1) conventional MCAR-T cells generated from healthy

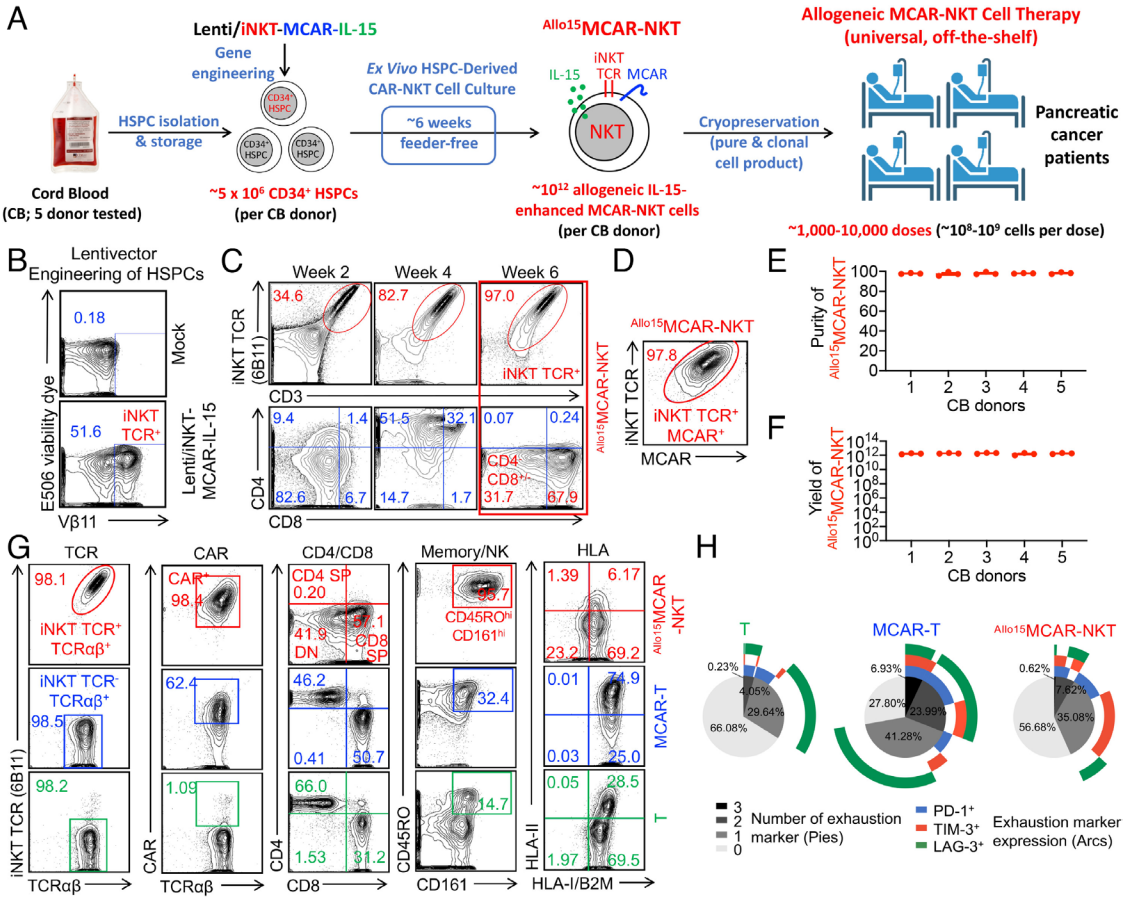

Fig. 1. Generation and characterization of HSPC-engineered allogeneic IL-15-enhanced MCAR-NKT (^{Allo15}MCAR-NKT) cells. (*A*) Schematics showing the generation of ^{Allo15}MCAR-NKT cells. HSPC, hematopoietic stem, and progenitor cells; Lenti/iNKT-MCAR-IL-15, lentiviral vector encoding a pair of iNKT TCR α and β chains, a mesothelin (MSLN)-directed CAR, and a human soluble IL-15. (*B*) FACS plots showing the transduction rate on CD34⁺ HSPCs at 72 h after lentivector transduction (n = 3). Intracellular iNKT TCR was stained using a TCR Vβ11 monoclonal antibody. (*C*) FACS monitoring of the generation of ^{Allo15}MCAR-NKT cells during the 6-week culture. iNKT TCR was stained using a 6B11 monoclonal antibody. (*D*) FACS detection of CAR expression on ^{Allo15}MCAR-NKT cells. MCAR was stained using a F(ab')2 antibody. (*E*) Purity of ^{Allo15}MCAR-NKT cells (identified as 6B11⁺CD3⁺MCAR⁺ cells; n = 3). 5 different cord blood (CB) donors were tested. (*F*) Yield of ^{Allo15}MCAR-NKT cells (n = 3). 5 different CB donors were tested. (*G*) FACS detection of surface marker expression of ^{Allo15}MCAR-NKT cells. Healthy donor peripheral blood mononuclear cell (PBMC)-derived conventional MCAR-engineered T (MACR-T) and quiescent T cells were included as controls. (*H*) SPICE analysis of exhaustion marker expression of the indicated therapeutic cells. Pie charts reflect proportions of indicated cell groups expressing indicated numbers (0 to 3) of exhaustion markers. Colored arcs indicate the specific combinations of exhaustion markers expressed. Representative of over 5 experiments. Data are presented as the mean ± SEM.

donor peripheral blood mononuclear cells (PBMCs), which are currently used in autologous CAR-T cell therapy and clinical trials (37–40); and 2) unstimulated, quiescent PBMC-derived T cells, included as a staining control.

In terms of surface phenotype, ^{Allo15}MCAR-NKT cells demonstrated several key distinctions. Notably, these cells are engineered using a single lentiviral vector encoding the invariant NKT TCR, a mesothelin-specific CAR, and human soluble IL-15, resulting in uniform CAR expression (~100%) across the population (Fig. 1*G* and *SI Appendix*, Fig. S1*C*). In contrast, conventional MCAR-T cells typically show variable CAR transduction efficiency, depending on the vector system (lentiviral or retroviral), donor T cell activation state, and culture conditions, which may result in inconsistent CAR expression and heterogeneous cell products (Fig. 1*G* and *SI Appendix*, Fig. S1 *C* and *D*).

Phenotypically, conventional MCAR-T cells predominantly exhibit either CD4⁺ or CD8⁺ SP profiles. In contrast, ^{Allo15}MCAR-NKT cells consist of both CD8⁺ SP and CD4⁻CD8⁻ DN populations (Fig. 1*G* and *SI Appendix*, Fig. S1*E*), consistent with NKT lineage characteristics. They also express high levels of CD45RO, a memory T cell marker, and CD161, a hallmark of NK lineage cells, both of which were significantly elevated compared to conventional CAR-T cells (Fig. 1*G* and *SI Appendix*, Fig. S1*F*). Interestingly, ^{Allo15}MCAR-NKT cells displayed substantially lower surface expression of HLA class I and II molecules (Fig. 1*G* and *SI Appendix*, Fig. S1*F*), suggesting an intrinsic ability to evade host T cell–mediated alloreactivity, thereby supporting their utility as an off-the-shelf, allogeneic cell therapy platform with reduced risk of allorejection (41–44).

In addition, exhaustion profiling revealed a markedly reduced frequency of PD-1⁺LAG-3⁺TIM-3⁺ triple-positive populations in ^{Allo15}MCAR-NKT cells compared to conventional MCAR-T cells (Fig. 1*H*). This suggests that ^{Allo15}MCAR-NKT cells possess a less exhausted, more durable phenotype, which may enhance their persistence and function in vivo (45, 46). Moreover, ^{Allo15}MCAR-NKT cells expressed higher levels of key activating NKRs, including CD56, NKG2D, DNAM-1, NKp30, and NKp44, compared to MCAR-T cells (*SI Appendix*, Fig. S1 *G* and *H*). Functional profiling by intracellular cytokine staining confirmed that ^{Allo15}MCAR-NKT cells produced elevated levels of proinflammatory cytokines (IFN-γ, TNF-α, and IL-2) and cytotoxic effector molecules (Perforin and Granzyme B), underscoring their robust antitumor potential (*SI Appendix*, Fig. S1 *G* and *H*).

Collectively, these findings demonstrate that ^{Allo15}MCAR-NKT cells possess a hybrid T/NK cell phenotype, with enhanced memory, activation, and cytolytic features, low exhaustion, and reduced immunogenicity. These properties support their strong therapeutic potential as an off-the-shelf, allogeneic immunotherapy platform for targeting solid tumors such as PC.

^{Allo15}MCAR-NKT Cells Directly Kill Pancreatic Tumor Cells at High Efficacy and CAR/NKR Dual Targeting Mechanism. To evaluate the in vitro antitumor activity of ^{Allo15}MCAR-NKT cells against PC, we conducted a series of tumor cell killing assays using a panel of tumor cell lines with diverse antigen expression profiles, molecular characteristics, and genetic backgrounds (Fig. 2*A*). This comprehensive approach enabled assessment of both CAR-dependent and CAR-independent cytotoxic mechanisms.

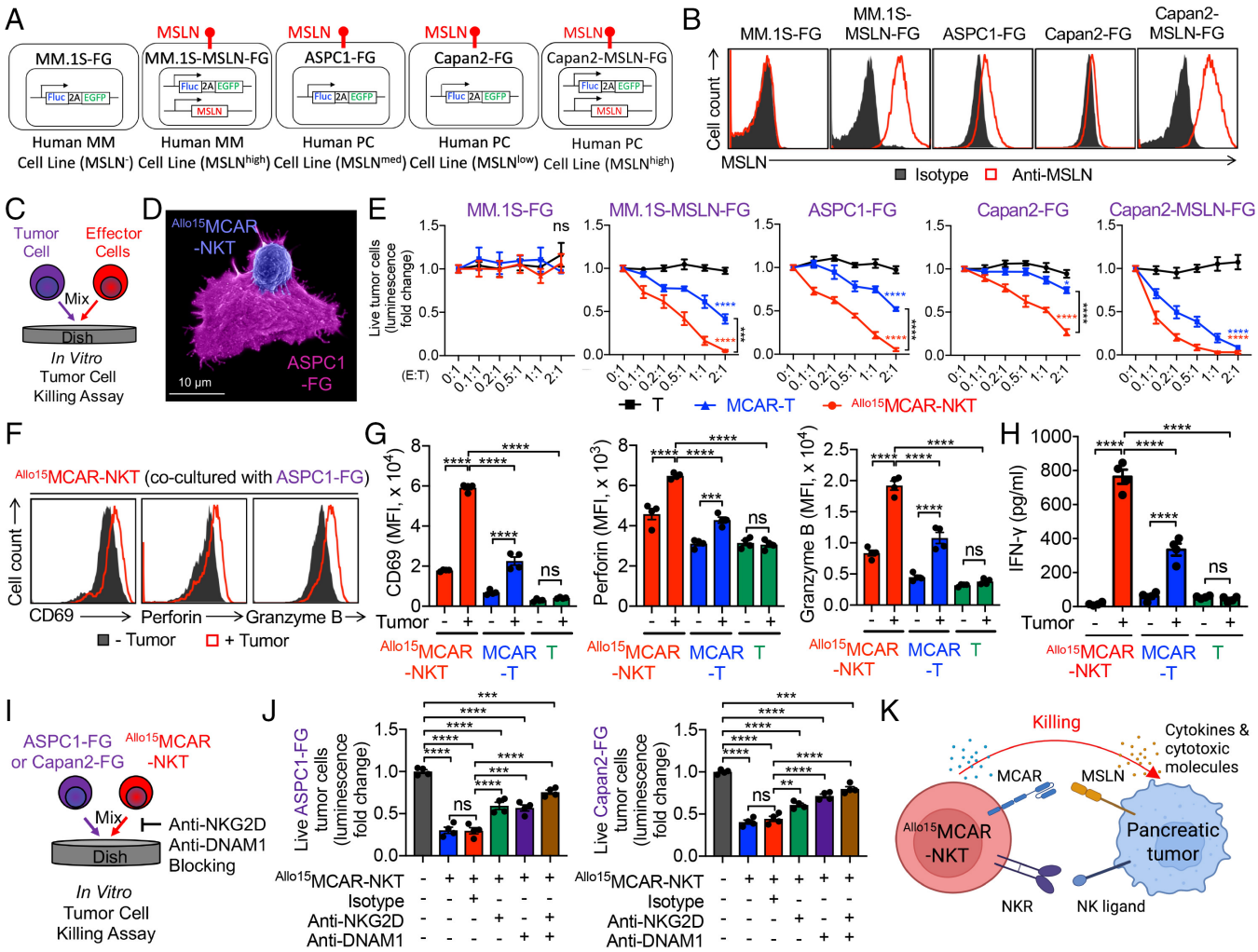

Fig. 2. In vitro tumor cell killing efficacy and mechanism of ^{Allo15}MCAR-NKT cells. (*A–E*) Studying the in vitro antitumor efficacy of ^{Allo15}MCAR-NKT cells against human multiple myeloma (MM) and pancreatic cancer (PC) cell lines. MCAR-T cells and non-MCAR-engineered PBMC-derived T cells were included as therapeutic cell controls. (*A*) Schematics showing the indicated human MM and PC cell lines. FG, firefly luciferase and enhanced green fluorescence protein (FG). MM.1S-FG, MM.1S cell engineered to overexpress FG; MM.1S-MSLN-FG, MM.1S-FG cell engineered to overexpress MSLN; ASPC1-FG, ASPC1 cell engineered to overexpress FG; Capan2-FG, Capan2 cell engineered to overexpress FG. Capan2-MSLN-FG, Capan2-FG cell engineered to overexpress MSLN. (*B*) FACS detection of MSLN expression on the indicated tumor cells. (*C*) Experimental design. (*D*) Scanning electron microscope (SEM) visualization of ^{Allo15}MCAR-NKT cells attacking PC tumor cells. (*E*) Tumor cell killing data at 24 h (n = 4). (*F–H*) Studying the expression of effector molecules of ^{Allo15}MCAR-NKT cells. (F) FACS detection of surface CD69 as well as intracellular Perforin and Granzyme B in ^{Allo15}MCAR-NKT cells. (*G*) Quantification of (*F*) (n = 4). (*H*) ELISA analyses of IFN-γ production in the indicated therapeutic cells (n = 4). (*I–K*) Studying the tumor cell killing mechanisms of ^{Allo15}MCAR-NKT cells mediated by NKRs (i.e., NKG2D and DNAM-1). (*I*) Experimental design. (*J*) Tumor cell killing data at 24 h (ASPC1-FG, E:T ratio = 1:1; Capan2-FG, E:T ratio = 2:1; n = 4). Representative of 3 experiments. Data are presented as the mean ± SEM. ns, not significant, **P* < 0.05, ***P* < 0.01, ****P* < 0.001, *****P* < 0.0001 by one-way ANOVA (*G*, *H*, and *J*), or two-way ANOVA (*E*).

We first compared the cytotoxic responses of ^{Allo15}MCAR-NKT cells against five tumor cell lines: two NK killing-resistant MM lines, MM.1S (MSLN$^-$) and MM.1S-MSLN (engineered to overexpress MSLN), as well as three NK killing-sensitive PC cell lines, ASPC1 (MSLN^{medium}), Capan2 (MSLN^{low}), and Capan2-MSLN (MSLN^{high}) (Fig. 2 *A* and *B*). All tumor lines were engineered to express firefly luciferase and green fluorescence protein dual reporters (FG), enabling quantitative analysis via bioluminescence imaging and flow cytometry (Fig. 2*A*). Three therapeutic cell groups were tested using an in vitro tumor cell killing assay, including ^{Allo15}MCAR-NKT, conventional MCAR-T, and T cells (Fig. 2*C*). Scanning electron microscopy (SEM) revealed direct interaction and engagement between ^{Allo15}MCAR-NKT cells and ASPC1-FG tumor cells in vitro (Fig. 2*D*).

As expected, unmodified T cells exhibited negligible cytotoxicity across all tumor lines (Fig. 2*E*). Conventional MCAR-T cells selectively eliminated MSLN$^+$ tumor cells, but had no effect on MSLN$^-$ targets, confirming the antigen-specific nature of their cytotoxic activity (Fig. 2*E*). In contrast, ^{Allo15}MCAR-NKT cells demonstrated robust killing of both MSLN$^+$ and MSLN$^-$ PC cells, indicating the use of dual CAR-dependent and CAR-independent mechanisms (Fig. 2*E*). Phenotypic analysis further showed enhanced activation of ^{Allo15}MCAR-NKT cells, as evidenced by upregulation of CD69 and increased production of effector cytokines (e.g., IFN-γ) and cytotoxic molecules (e.g., Perforin and Granzyme B) compared to MCAR-T cells (Fig. 2 *F–H*).

To dissect the CAR-independent component of cytotoxicity, we performed NKR blocking assays using neutralizing antibodies targeting NKG2D and DNAM-1 (Fig. 2*I*). Inhibition of these NKRs significantly reduced the cytolytic activity of ^{Allo15}MCAR-NKT cells (Fig. 2*J*), confirming that their NKR-mediated tumor recognition contributes critically to antigen-independent killing (Fig. 2*K*).

To model tumor antigen escape, a major limitation of conventional CAR-T therapies (47, 48), we generated a heterogeneous Capan2 tumor population containing a mixture of MSLN$^+$ and MSLN$^-$ cells (*SI Appendix*, Fig. S2*A*). MCAR-T cells selectively cleared the MSLN$^+$ subpopulation while failing to eliminate MSLN$^-$ tumor cells (*SI Appendix*, Fig. S2 *B* and *C*). In contrast,

^{Allo15}MCAR-NKT cells effectively eliminated both populations, demonstrating their ability to overcome tumor heterogeneity and antigen-loss variants through multimodal targeting (*SI Appendix*, Fig. S2 *B* and *C*).

We next assessed the long-term cytolytic capacity of ^{Allo15}MCAR-NKT cells using an in vitro serial tumor cell killing assay, in which fresh tumor cells were added every two days over a 20-day period (*SI Appendix*, Fig. S2*D*). ^{Allo15}MCAR-NKT cells maintained sustained cytotoxic activity against both MSLN$^+$ and MSLN$^-$ tumor cells throughout the entire assay, whereas MCAR-T cells showed progressive loss of function (*SI Appendix*, Fig. S2*E*). This durable activity of ^{Allo15}MCAR-NKT cells may be attributed to their persistent effector function, strong cytolytic potential, and reduced exhaustion phenotype (Figs. 1*H* and 2 *F*–*H* and *SI Appendix*, Fig. S1 *G* and *H*).

Collectively, these findings highlight the potent, durable, and multifaceted antitumor activity of ^{Allo15}MCAR-NKT cells. Their ability to engage tumors through both CAR and NKR pathways, and to eliminate antigen-low and heterogeneous tumor populations, supports their potential as a next-generation allogeneic immunotherapy for the treatment of PC and other solid tumors with high antigenic variability.

^{Allo15}MCAR-NKT Cells Surpass CAR-Engineered NK Cells in Sustained Antitumor Efficacy. Since ^{Allo15}MCAR-NKT cells express high levels of NKRs and can eliminate tumor cells through NKR-mediated mechanisms, we next compared their in vitro tumor cell killing capacity with that of CAR-engineered NK cells. To this end, we generated human PBMC-derived, IL-15-enhanced, MCAR-engineered NK cells (^{PBMC15}MCAR-NK) and conducted side-by-side comparisons with ^{Allo15}MCAR-NKT cells (*SI Appendix*, Fig. S3*A*).

To generate ^{PBMC15}MCAR-NK cells, CD56$^+$ NK cells were isolated from healthy donor PBMCs using MACS, stimulated with artificial APCs, and transduced with a lentiviral vector encoding both MCAR and human IL-15, achieving a transduction efficiency of ~30% (*SI Appendix*, Fig. S3 *A* and *B*). Although CAR expression was stable, the overall expansion capacity of ^{PBMC15}MCAR-NK cells was limited, with only a 3 to 5-fold increase observed over a one-week culture period (*SI Appendix*, Fig. S3*C*). This low proliferative potential may limit the feasibility of using these cells as an off-the-shelf therapeutic product for treating multiple cancer patients.

The antitumor efficacy of two therapeutic cells was then evaluated using both in vitro short-term tumor cell killing assays and long-term serial tumor cell killing assays (*SI Appendix*, Fig. S3 *D* and *F*). In the 24-hour tumor cell killing assay, both cell products demonstrated comparable and robust cytotoxicity against MSLN$^+$ ASPC1-FG and Capan2-MSLN-FG, as well as MSLN$^-$ Capan2-FG human PC cell lines (*SI Appendix*, Fig. S3*E*). These findings suggest that both therapeutic cell types effectively eliminate tumor cells through a combination of CAR-dependent and CAR-independent, NKR-mediated mechanisms. However, in the long-term assay, ^{Allo15}MCAR-NKT cells demonstrated superior tumor cell killing and more durable tumor control, indicating enhanced persistence and sustained antitumor activity compared to ^{PBMC15}MCAR-NK cells (*SI Appendix*, Fig. S3*G*). Together, these results highlight the unique advantage of ^{Allo15}MCAR-NKT cells in achieving long-term tumor control, underscoring their potential as a more effective and scalable off-the-shelf cell therapy platform than PBMC-derived CAR-NK cells.

^{Allo15}MCAR-NKT Cells Exhibit Enhanced in Vivo Antitumor Efficacy in an Orthotopic Human PC Model. To evaluate the in vivo antitumor efficacy of ^{Allo15}MCAR-NKT cells, we employed a series of human PC xenograft mouse models. We first established an orthotopic PC model, in which human tumor cells were implanted directly into the pancreas of NSG mice, thereby more accurately recapitulating the anatomical context and metastatic potential observed in clinical PC (Fig. 3*A*) (49).

Two types of therapeutic immune cells were administered via intravenous injection, including ^{Allo15}MCAR-NKT cells and conventional MCAR-T cells (Fig. 3*A*). Both cell types exerted antitumor activity and were capable of suppressing tumor progression (Fig. 3 *B* and *C*). However, mice treated with ^{Allo15}MCAR-NKT cells demonstrated significantly greater tumor control, as reflected by markedly lower tumor bioluminescent imaging (BLI) signals, indicating superior tumor clearance (Fig. 3 *B* and *C* and *SI Appendix*, Fig. S4*A*).

To investigate the basis for this enhanced efficacy, we examined the in vivo biodistribution of the therapeutic cells. ^{Allo15}MCAR-NKT cells preferentially homed to the pancreatic tumor site, with limited distribution to nontarget tissues such as the liver, lungs, spleen, and peripheral blood (Fig. 3 *D* and *E*). In contrast, while MCAR-T cells were also detected in the pancreas, a substantial proportion accumulated in off-target organs—particularly the liver, where the highest frequency of MCAR-T cells was observed (Fig. 3 *D* and *E*). These findings suggest that ^{Allo15}MCAR-NKT cells possess superior tumor-homing and tissue-infiltrating capabilities, potentially contributing to their enhanced antitumor effects.

We next performed immunohistochemical (IHC) analyses to evaluate intratumoral infiltration. Although MCAR-T cells were present in the pancreas, they primarily localized to the peritumoral region, showing minimal penetration into the tumor mass itself (Fig. 3 *F* and *G*). In contrast, ^{Allo15}MCAR-NKT cells exhibited robust infiltration into the tumor core, with clear colocalization with tumor cells (Fig. 3 *F* and *G*). These results indicate that ^{Allo15}MCAR-NKT cells can effectively navigate and penetrate the tumor microenvironment, a key feature for successful immunotherapy in solid tumors.

To elucidate the molecular mechanisms underlying the observed differences in trafficking, we compared the chemokine receptor expression profiles of ^{Allo15}MCAR-NKT cells and conventional MCAR-T cells. ^{Allo15}MCAR-NKT cells displayed markedly elevated expression of tumor-homing receptors such as CCR2, CCR5, CCR6, CXCR3, and CXCR4, all of which are implicated in directing effector lymphocytes into inflamed and tumor-infiltrated tissues (*SI Appendix*, Fig. S4 *B* and *C*) (50–52). In contrast, ^{Allo15}MCAR-NKT cells expressed lower levels of CCR7, a chemokine receptor associated with migration to secondary lymphoid organs (*SI Appendix*, Fig. S4 *B* and *C*) (53–55). This unique chemokine receptor repertoire likely underpins the enhanced tumor homing and infiltration of ^{Allo15}MCAR-NKT cells, while the reduced tumor presence of MCAR-T cells may be attributable to their preferential retention within peripheral lymphoid niches.

We also characterized the phenotype and functional status of the infiltrating therapeutic cells. Compared to MCAR-T cells, ^{Allo15}MCAR-NKT cells expressed significantly higher levels of activation and effector markers, including CD69, CD25, IFN-γ, Perforin, and Granzyme B, indicating a heightened cytotoxic state (Fig. 3*H*). In parallel, they exhibited markedly reduced expression of exhaustion markers such as PD-1, CTLA-4, TIM-3, LAG-3, and TIGIT, suggesting improved functional persistence and resistance to tumor-induced dysfunction (Fig. 3*I*).

Consistent with in vitro findings, ^{Allo15}MCAR-NKT cells maintained lower expression of HLA class I and class II molecules relative to MCAR-T cells (Figs. 1*G* and 3*J* and *SI Appendix*, Fig. S1*F*). This feature likely contributes to their reduced immunogenicity and enhanced resistance to host T cell–mediated allorejection, supporting their application as an off-the-shelf allogeneic therapy.

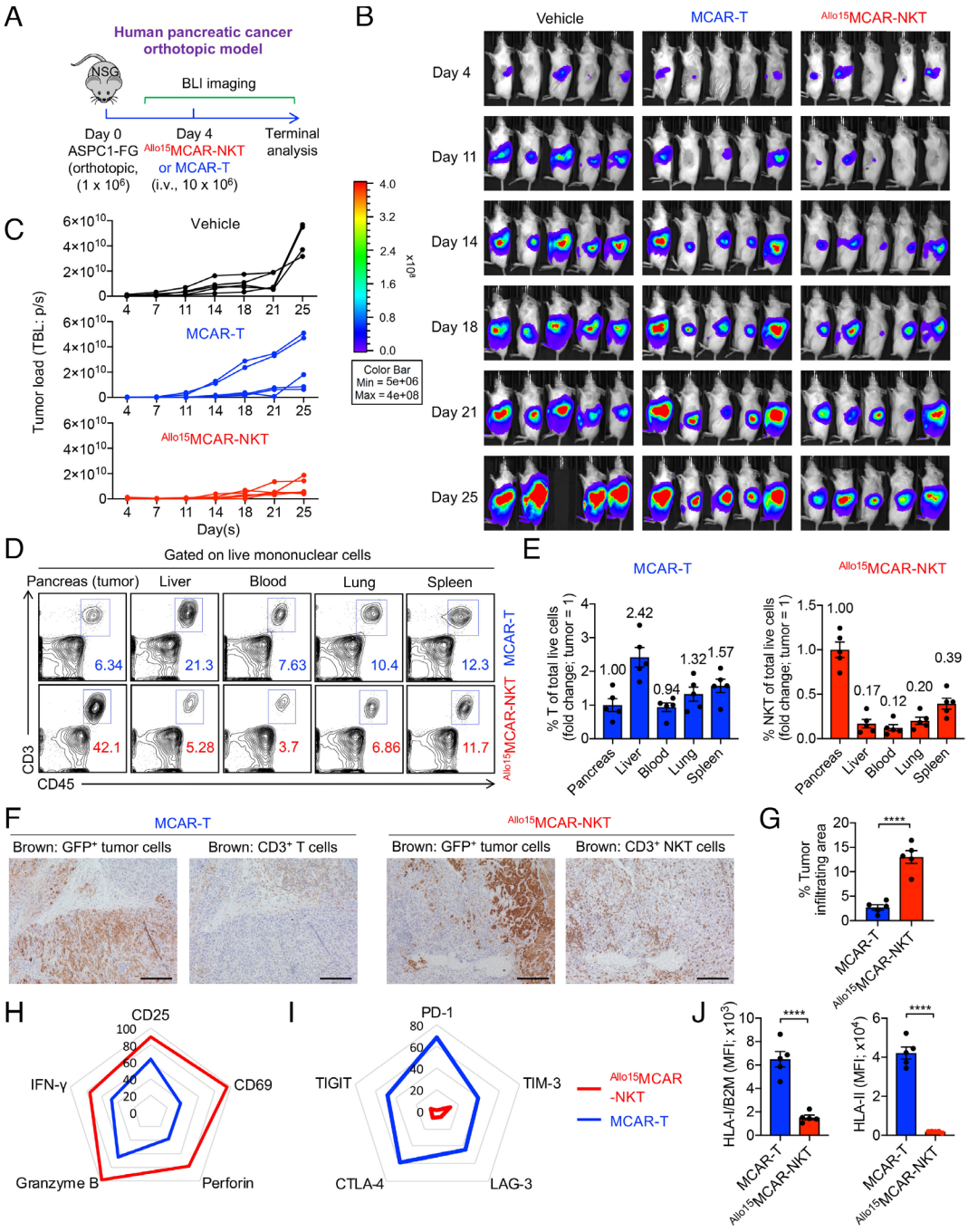

Fig. 3. In vivo antitumor efficacy of ^{Allo15}MCAR-NKT cells against orthotopic PC. (*A*) Experimental design. BLI, live animal bioluminescence imaging. (*B*) BLI images measuring tumor loads in experimental mice over time. (*C*) Quantification of (B) (n = 5). (*D*) FACS analyses of $CD3^+CD45^+$ double positive T or NKT cells in mouse tissues on Day 25. (*E*) Quantification of (*D*) (n = 5). The percentage of therapeutic cells was measured across various tissues. The value in the pancreas tissue was set as 1, and the percentages in other tissues were normalized by dividing by the pancreatic value. (*F*) Immunohistochemical (IHC) staining showing GFP^+ tumor cells and $CD3^+$ T or NKT cells in the pancreas of experimental mice. Tissue samples were collected on day 25. (Scale bar, 200 μm.) (*G*) Quantification of T or NKT cell infiltrating area (n = 5). The value was calculated by measuring the percentage of $CD3^+$ area within the GFP^+ tumor cell area. (*H* and *I*) Radar plots showing the expression of activation and effector markers (*H*), and immune checkpoint molecules (*I*) on the therapeutic cells. Data represent the percentage of positive cells as measured by flow cytometry, with each value calculated as the mean from five experimental mice. (*J*) FACS analyses the surface expression of HLA-I and HLA-II molecules on ^{Allo15}MCAR-NKT and MCAR-T cells (n = 5). Representative of 2 experiments. Data are presented as the mean ± SEM. ****$P < 0.0001$ by Student's *t* test (*G* and *J*).

In conclusion, ^{Allo15}MCAR-NKT cells demonstrate superior in vivo antitumor efficacy against orthotopic pancreatic tumors. This is driven by enhanced tumor homing and infiltration, potent effector function, reduced exhaustion, and low immunogenicity—highlighting their strong translational potential as an allogeneic cellular immunotherapy for PC.

^{Allo15}MCAR-NKT Cells Demonstrate Superior In Vivo Therapeutic Activity Against Metastatic Human PC. PC metastasis presents a major clinical challenge, as PC frequently disseminates to distant organs such as the lungs, liver, bone marrow, and peritoneum. These metastatic lesions contribute significantly to disease progression, treatment resistance, and poor patient prognosis (56, 57). Therefore, effectively targeting metastatic disease is critical for advancing curative immunotherapeutic strategies for PC.

To model metastatic disease, we established a disseminated human PC xenograft model, in which ASPC1-FG tumor cells were intravenously injected into NSG mice (Fig. 4*A*). These tumor cells predominantly colonized the lungs, with limited spread to secondary sites including the liver, bone marrow, and pancreas, providing a relevant preclinical system to assess the antitumor efficacy of therapeutic cells in a metastatic setting (Fig. 4*B* and *SI Appendix*, Fig. S4*B*).

Tumor-bearing mice were treated with either ^{Allo15}MCAR-NKT cells or conventional MCAR-T cells via intravenous injection. While both therapies resulted in tumor burden reduction, ^{Allo15}MCAR-NKT cells achieved superior tumor control, as demonstrated by significantly lower tumor bioluminescence signals and prolonged overall survival (Fig. 4 *B*–*D*). Notably, biodistribution analysis revealed that ^{Allo15}MCAR-NKT cells preferentially trafficked to the lungs, the primary site of tumor burden in this model (Fig. 4 *E* and *F*). This observation underscores their

enhanced tumor-homing ability, which may be attributed to their distinct chemokine receptor expression profile, enabling more effective localization to tumor sites (20).

Consistent with findings from the orthotopic model, ^{Allo15}MCAR-NKT cells in the metastatic setting exhibited elevated expression of activation and cytotoxic markers, including CD25, CD69, IFN-γ, Perforin, and Granzyme B, and reduced levels of exhaustion markers such as PD-1, TIM-3, and LAG-3, relative to MCAR-T cells (Fig. 4 *G* and *H*). These functional advantages likely contribute to their sustained antitumor activity. Moreover, ^{Allo15}MCAR-NKT cells retained low expression of HLA class I and class II molecules (Fig. 4*I*), a feature that reduces their visibility to host alloreactive T cells and supports their immune evasion and persistence in allogeneic settings. This immunologically silent profile further reinforces the suitability of ^{Allo15}MCAR-NKT cells as a universal, off-the-shelf cell therapy for metastatic PC.

^{Allo15}MCAR-NKT Cells Effectively Counteract CAR Antigen Escape. The ability of ^{Allo15}MCAR-NKT cells to engage tumor cells through both CAR-dependent and CAR-independent mechanisms enables them to effectively counteract tumor antigen escape. To investigate this capability in vivo, we established two subcutaneous xenograft models using Capan2-FG (MSLN$^-$) and Capan2-MSLN-FG (MSLN$^+$) PC cells, representing CAR antigen-negative and CAR antigen-positive tumors, respectively (Fig. 5 *A* and *E*). Tumor cells were subcutaneously injected into NSG mice, and therapeutic cells, including ^{Allo15}MCAR-NKT and conventional MCAR-T cells, were delivered via peritumoral injection to facilitate direct interaction with tumor cells and allow for precise assessment of antigen-specific and antigen-independent antitumor activity (Fig. 5 *A* and *E*).

As expected, conventional MCAR-T cells effectively suppressed tumor growth in the MSLN$^+$ (Capan2-MSLN-FG) model but failed to control tumors in the MSLN$^-$ (Capan2-FG) model, consistent with their strict CAR-dependent cytotoxicity (Fig. 5 *B–D* and *F–H*). In contrast, ^{Allo15}MCAR-NKT cells demonstrated potent antitumor activity in both models, confirming their ability to eliminate tumor cells through CAR-independent mechanisms, likely mediated by their NKR-based recognition pathways (Fig. 5 *B–D* and *F–H*). These results underscore the therapeutic advantage of ^{Allo15}MCAR-NKT cells in addressing tumor heterogeneity and antigen escape.

Biodistribution analysis further revealed that ^{Allo15}MCAR-NKT cells remained localized at the tumor site, with minimal migration to peripheral organs (Fig. 5 *I* and *J*). In contrast, conventional MCAR-T cells were broadly distributed, particularly accumulating in the liver, spleen, and lungs (Fig. 5 *I* and *J*). This widespread infiltration by MCAR-T cells may reflect their xenogeneic GvHD potential, a phenomenon commonly observed in preclinical studies involving human T cells in immunodeficient mice (58).

Phenotypic analysis of tumor-infiltrating ^{Allo15}MCAR-NKT cells showed elevated CD69 expression, indicative of activation, and low PD-1 expression, suggesting resistance to exhaustion (Fig. 5 *K* and *L*). Moreover, these cells exhibited low surface expression of HLA class I and II molecules, associated with reduced immunogenicity and resistance to host-mediated allorejection (Fig. 5 *M* and *N*). Together, these findings highlight the unique advantage of ^{Allo15}MCAR-NKT cells in targeting antigen-heterogeneous tumors while minimizing off-target effects and immunotoxicity.

^{Allo15}MCAR-NKT Cells Resist Host Cell–Mediated Allorejection and Do Not Induce GvHD. The low surface expression of HLA class I and II molecules on ^{Allo15}MCAR-NKT cells, along with their stable expression both in vitro and in vivo postinfusion (Figs. 1*G*, 3*J*, 4*I*, and 5 *M* and *N*), positions these cells as a promising allogeneic immunotherapy platform with inherent resistance to host T cell–mediated allorejection. To assess this potential, we performed an in vitro mixed lymphocyte reaction (MLR) assay, in which allogeneic PBMCs from mismatched donors served as responders, and irradiated ^{Allo15}MCAR-NKT cells or conventional MCAR-T cells were used as stimulators (*SI Appendix,* Fig. S5*A*).

As anticipated, conventional MCAR-T cells elicited robust IFN-γ production of allogeneic PBMCs, indicative of strong immunogenicity and susceptibility to rejection (*SI Appendix,* Fig. S5*B*). In contrast, ^{Allo15}MCAR-NKT cells induced significantly reduced T cell activation across all five donor PBMC samples tested (*SI Appendix,* Fig. S5*B*), demonstrating their hypoimmunogenic phenotype and enhanced ability to evade alloreactive immune responses (41, 59). Importantly, the low expression of HLA-I/II molecules on ^{Allo15}MCAR-NKT cells was intrinsic and remained stable under proinflammatory conditions, including IFN-γ stimulation in vitro and within the tumor microenvironment in vivo (Figs. 1*G*, 3*J*, 4*I*, and 5 *M* and *N* and *SI Appendix,* Fig. S5 *C* and *D*). These data suggest that ^{Allo15}MCAR-NKT cells possess a stable, immune-evasive profile that minimizes recognition by host immune cells, supporting their feasibility as an off-the-shelf therapeutic product (*SI Appendix,* Fig. S5*E*).

Given the allogeneic nature of this approach, the potential to induce GvHD is a critical safety concern, as GvHD arises when infused donor-derived T cells recognize and attack host tissues (60). However, NKT cells are uniquely restricted by the nonpolymorphic CD1d molecule, rather than classical MHC molecules, and therefore are not expected to initiate GvHD responses—a concept supported by prior preclinical and clinical studies (15, 43, 61, 62). To evaluate the risk of GvHD, we first performed an in vitro MLR assay in which irradiated, donor-mismatched PBMCs served as stimulators, and either ^{Allo15}MCAR-NKT or conventional MCAR-T cells were included as responders (*SI Appendix,* Fig. S5*F*). Consistent with expectations, MCAR-T cells demonstrated high levels of responder activation (IFN-γ production), indicative of graft-versus-host (GvH) reactivity, whereas ^{Allo15}MCAR-NKT cells exhibited minimal GvH responses (*SI Appendix,* Fig. S5*G*).

To further assess GvHD potential in vivo, we employed a humanized xenograft NSG mouse model (*SI Appendix,* Fig. S5*H*). Mice treated with conventional MCAR-T cells rapidly developed signs of severe xenogeneic GvHD, including marked weight loss, GvHD-associated symptoms, and eventual mortality (*SI Appendix,* Fig. S5 *I-K*). In stark contrast, mice treated with ^{Allo15}MCAR-NKT cells remained GvHD-free, maintaining stable body weight and long-term survival throughout the study period (*SI Appendix,* Fig. S5 *I-K*). These findings underscore the safety profile of ^{Allo15}MCAR-NKT cells and their lack of GvHD-inducing potential.

^{Allo15}MCAR-NKT Cells Induce Less Cytokine Release Syndrome (CRS) Toxicity. CRS is a common toxicity associated with conventional CAR-T cell therapy, largely driven by excessive activation of infused CAR-T cells and the resulting systemic release of proinflammatory cytokines, which can lead to fever, hypotension, and multiorgan dysfunction (63, 64). We then evaluated CRS-associated toxicity and measured the corresponding in vivo cytokine levels for ^{Allo15}MCAR-NKT cells and conventional MCAR-T cells.

We first assessed the potential for CRS toxicity induced by ^{Allo15}MCAR-NKT cells using an ASPC1-FG human PC xenograft model in NSG mice (*SI Appendix,* Fig. S5*L*). High doses of tumor cells were administered intraperitoneally (i.p.), followed by a high-dose i.p. injection of therapeutic cells (*SI Appendix,* Fig. S5*L*). This i.p. model was adapted from a previously reported xenograft system for studying CAR-T cell–induced CRS, in which human CAR-T cells interact with mouse peritoneal macrophages to exacerbate CRS-like

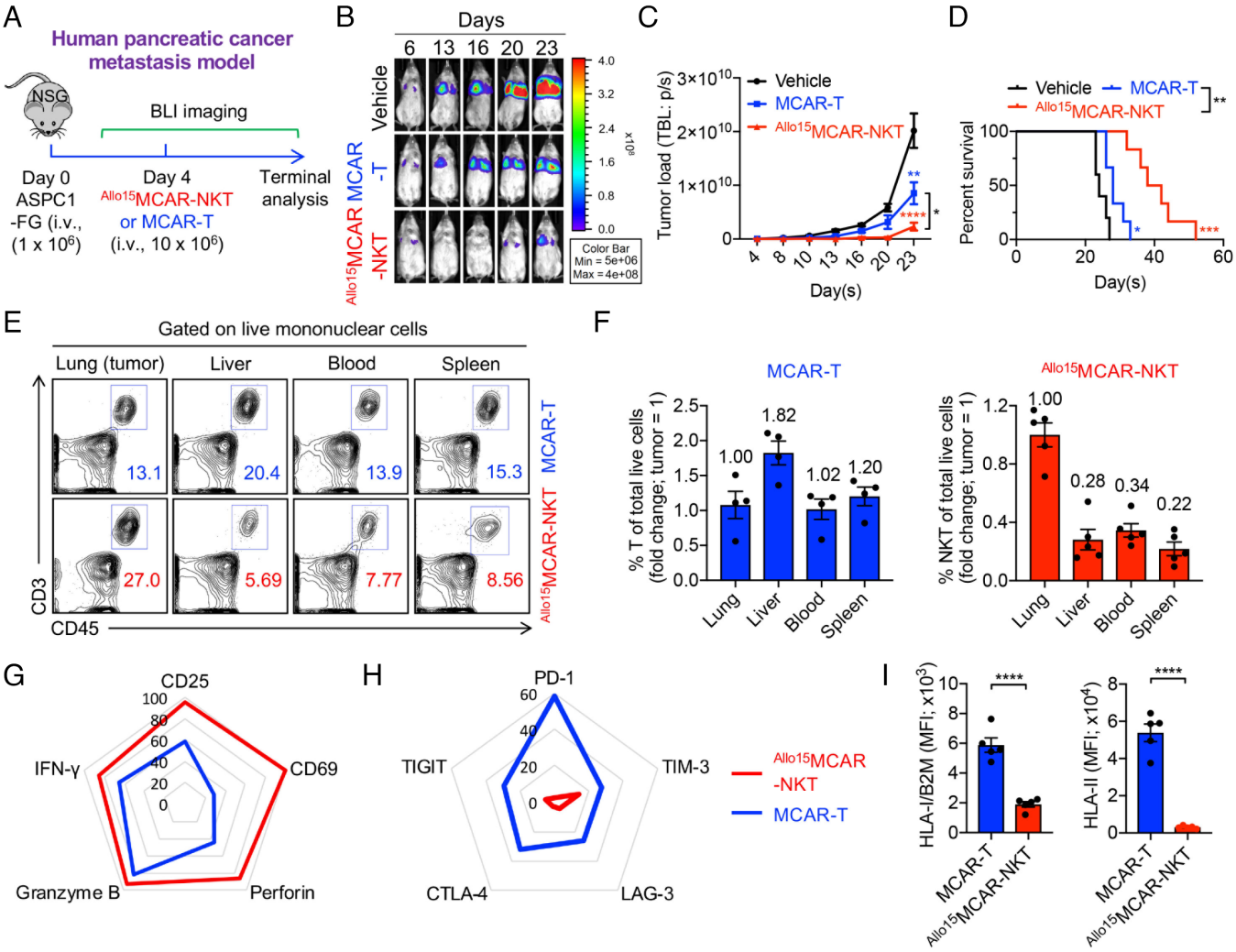

Fig. 4. In vivo antitumor efficacy of ^{Allo15}MCAR-NKT cells against metastatic PC. (*A*) Experimental design. (*B*) BLI images measuring tumor loads in experimental mice over time. (*C*) Quantification of (*B*) (n = 5 to 6). (*D*) Kaplan–Meier survival curves (n = 5 to 6). (*E*) FACS analyses of $CD3^+CD45^+$ double positive T or NKT cells in mouse tissues 30 d post injection of therapeutic cells. (*F*) Quantification of (*E*) (n = 4 or 5). The percentage of therapeutic cells was measured across various tissues. The value in the lung (tumor) tissue was set as 1, and the percentages in other tissues were normalized by dividing by the lung value. (*G* and *H*) Radar plots showing the expression of activation and effector markers (*G*), and immune checkpoint molecules (*H*) on the therapeutic cells. Data represent the percentage of positive cells as measured by flow cytometry, with each value calculated as the mean from four or five experimental mice. (*I*) FACS analyses the surface expression of HLA-I and HLA-II molecules on ^{Allo15}MCAR-NKT and MCAR-T cells (n = 5). Representative of 2 experiments. Data are presented as the mean ± SEM. **P* < 0.05, ***P* < 0.01, ****P* < 0.001, *****P* < 0.0001, by Student's *t* test (*I*), one-way ANOVA (*C*; Data from day 23 were analyzed), or log rank (Mantel-Cox) test adjusted for multiple comparisons (*D*).

toxicity (65). In this model, ^{Allo15}MCAR-NKT cells induced significantly lower levels of CRS-related toxicity compared with conventional MCAR-T cells, as evidenced by more stable body weight and markedly lower levels of CRS-associated biomarkers, including mouse IL-6 and serum amyloid A-3 (SAA-3), in the serum (*SI Appendix,* Fig. S5 *M* and *N*). Analysis of human cytokines showed comparable levels of effector cytokines, including IFN-γ, TNF-α, and IL-2, while human IL-6 levels were significantly lower in ^{Allo15}MCAR-NKT–treated mice (*SI Appendix,* Fig. S5*O*). These findings suggest that ^{Allo15}MCAR-NKT cells may reduce the risk of CRS-like responses without compromising antitumor effector function. This favorable safety profile is likely attributable to their innate-like NK cell characteristics (Fig. 2 *I–K* and *SI Appendix,* Fig. S1 *G* and *H*) and their capacity to engage and modulate mouse macrophages (*SI Appendix,* Fig. S5*P*), thereby mitigating CRS amplification.

Discussion

Here, we developed a clinically adaptable platform to generate ^{Allo15}MCAR-NKT cells from CB $CD34^+$ HSPCs using a feeder-free differentiation protocol (28). This approach yielded highly pure (>97%), CAR^+/NKT TCR^+ cell populations with consistent yield, phenotype, and functionality across donors (Fig. 1). ^{Allo15}MCAR-NKT cells exhibited a hybrid T/NK profile characterized by high expression of NKRs, strong effector programs, and reduced expression of exhaustion markers relative to PBMC-derived conventional MCAR-T cells (Figs. 1 and 2). These features suggest a functionally potent and less exhausted cell product, well suited for targeting solid tumors.

Conventional CAR-T cells often show rapid exhaustion and limited tumor lysis in the PC microenvironment, which is shaped by suppressive myeloid cells and chronic inflammation (66). These issues result in low persistence, insufficient tumor control, and failure to overcome immune escape (66). In our study, ^{Allo15}MCAR-NKT cells exhibited superior cytotoxicity across multiple PC cell lines, outperforming conventional MCAR-T cells in both $MSLN^+$ and $MSLN^{low}$ tumor settings (Fig. 2*E*). Their killing activity was enhanced by dual recognition through CAR and NKRs and was attenuated upon blockade of NKG2D and DNAM-1, confirming the importance of these innate pathways

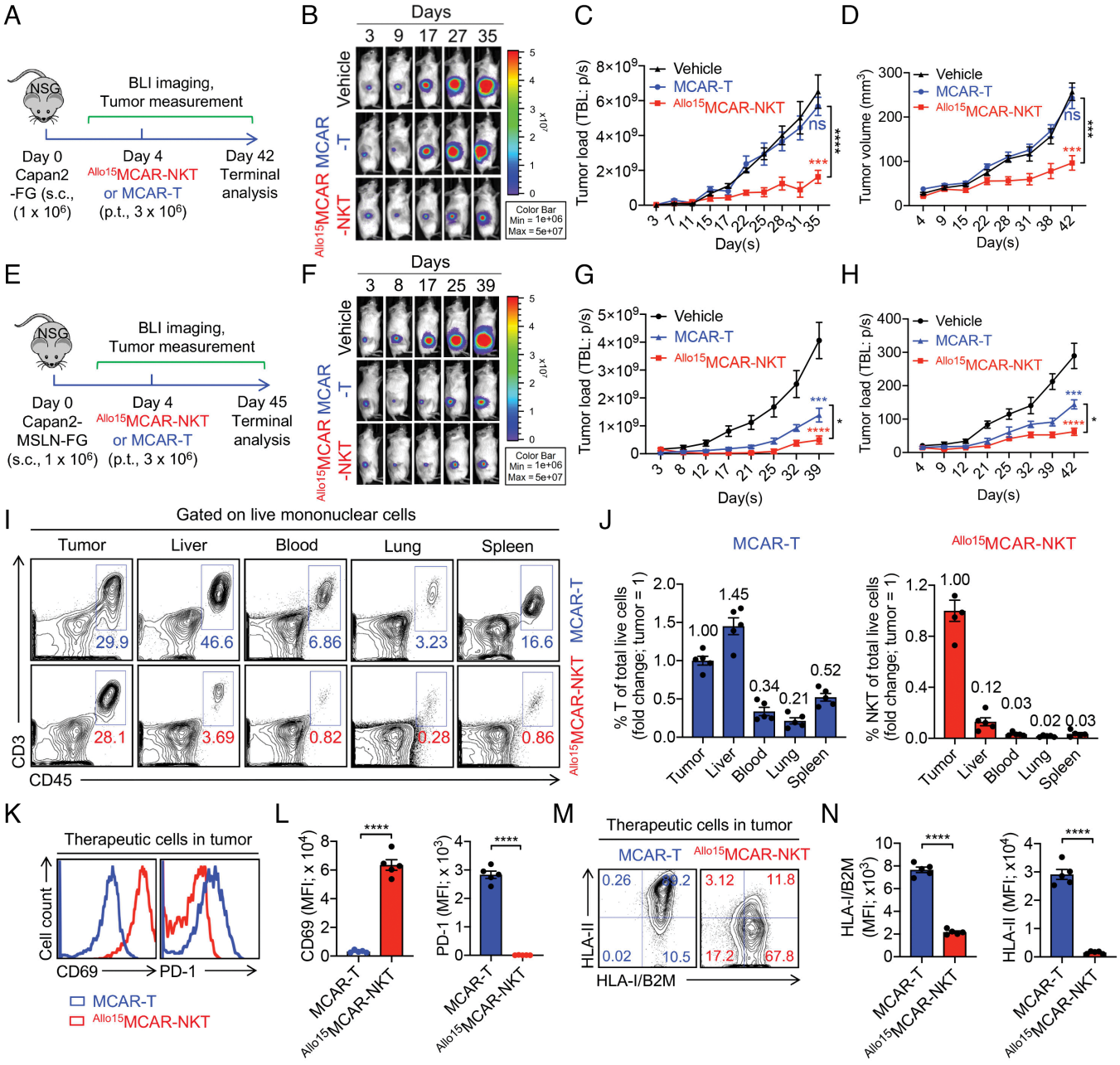

Fig. 5. In vivo antitumor efficacy of ^{Allo15}MCAR-NKT cells against PC with CAR antigen escape. (*A–D*) Studying the in vivo antitumor efficacy of ^{Allo15}MCAR-NKT cells using a Capan2-FG subcutaneous xenograft mouse model. This model is designed to mimic a low CAR antigen expression or antigen escape scenario. (*A*) Experimental design. (*B*) BLI images measuring tumor loads in experimental mice over time. (*C*) Quantification of (*B*) (n = 5). (*D*) Tumor size measurements over time (n = 5). (*E–N*) Studying the in vivo antitumor efficacy of ^{Allo15}MCAR-NKT cells using a Capan2-MSLN-FG subcutaneous xenograft mouse model. (*E*) Experimental design. (*F*) BLI images measuring tumor loads in experimental mice over time. (*G*) Quantification of (*F*) (n = 5). (*H*) Tumor size measurements over time (n = 5). (*I*) FACS analyses of $CD3^+CD45^+$ double positive T or NKT cells in mouse tissues 45 d post injection of therapeutic cells. (*J*) Quantification of (*I*) (n = 5). The percentage of therapeutic cells was measured across various tissues. The value in the tumor tissue was set as 1, and the percentages in other tissues were normalized by dividing by the tumor value. (*K*) FACS detection of CD69 and PD-1 expression on ^{Allo15}MCAR-NKT cells. (*L*) Quantification of (K) (n = 5). (*M*) FACS detection of HLA-I and HLA-II expression on ^{Allo15}MCAR-NKT cells. (*N*) Quantification of (*M*) (n = 5). Representative of 2 experiments. Data are presented as the mean ± SEM. ns, not significant, $*P < 0.05$, $***P < 0.001$, $****P < 0.0001$, by Student's *t* test (*L* and *N*), one-way ANOVA (*C*, *D*, *G*, and *H*; Data from the final day of the experiment were analyzed).

(Fig. 2*J*). Unlike MCAR-T cells, ^{Allo15}MCAR-NKT cells resisted antigen escape by eliminating both $MSLN^+$ and $MSLN^-$ tumor populations in coculture assays and retained long-term cytotoxic capacity in serial tumor challenge experiments (Fig. 2 *M–P*).

A defining barrier to cell therapy in PC is the poor infiltration of effector cells into tumor tissue. Stromal density and tumor-associated fibroblasts act as physical and biochemical barriers to therapeutic cell entry (66). As frequently seen in clinical biopsies and mouse models, even activated CAR-T cells often accumulate in peritumoral regions rather than penetrating the tumor core (67, 68). In our orthotopic PC models, ^{Allo15}MCAR-NKT cells achieved significantly stronger tumor control than MCAR-T cells, as evidenced by reduced tumor burden and enhanced therapeutic cell accumulation within the pancreas tumor area (Fig. 3 *B–E*). Immunohistochemical analyses further confirmed robust $CD3^+$ infiltration into the tumor core (Fig. 3*F*), and flow cytometry demonstrated sustained activation with low PD-1 and preserved effector function (Fig. 3*H*). Importantly, ^{Allo15}MCAR-NKT cells maintained low expression of HLA class I/II molecules (Fig. 3*J*), a property that may reduce host immune rejection in allogeneic

settings and support prolonged in vivo persistence. Together, these findings highlight the multimodal antitumor potential of ^{Allo15}MCAR-NKT cells, capable of targeting heterogeneous, immune-evasive, and immunosuppressive PC.

The management of metastatic PC remains a clinical dead end, as disseminated lesions in the lungs and liver are largely refractory to chemotherapy and immunotherapy (3, 66, 69). Even with aggressive treatment, metastatic spread drives most patient deaths, and therapeutic strategies that can target both primary and distal tumors are urgently needed. ^{Allo15}MCAR-NKT cells also exhibited potent activity in a PC metastasis model. Compared to MCAR-T cells, they achieved superior tumor reduction, prolonged survival, and greater infiltration into tumor-bearing lungs (Fig. 4 *C–F*). Therapeutic cells retained a highly activated, cytotoxic phenotype with minimal exhaustion (Fig. 4 *G-H*), and low HLA expression under the proinflammatory TME (Fig. 4*I*), further supporting their potential for immune evasion and sustained persistence in allogeneic settings.

Antigen escape remains a major mechanism of tumor relapse in CAR-based therapies. In PC, MSLN expression is variable and can be downregulated under therapeutic pressure. In clinical trials, relapses have been linked to selective outgrowth of MSLN$^-$ tumor subclones, limiting the durability of MSLN-redirected CAR-T cell responses (70). To mimic this challenge, we tested ^{Allo15}MCAR-NKT cells in Capan2 subcutaneous tumor models with either MSLN$^-$ or MSLN$^+$ tumors (Fig. 5). In both cases, ^{Allo15}MCAR-NKT cells effectively controlled tumor growth, outperforming MCAR-T cells and maintaining high tumor infiltration and effector marker expression (Fig. 5 *B–L*). Their ability to persist, remain functional, and localize within tumors despite CAR antigen variability underscores their potential to overcome antigen escape—a major limitation in current CAR-T therapies for solid tumors.

Safety and host cell–mediated allorejection remain major bottlenecks in the translation of allogeneic CAR therapies. Alloreactivity and HLA mismatch pose life-threatening risks, especially in inflamed tumor environments like PC. Compared to conventional MCAR-T cells, ^{Allo15}MCAR-NKT cells elicited significantly lower levels of IFN-γ production by allogeneic responder T cells, indicating reduced immunogenic potential (*SI Appendix,* Fig. S5*B*). Notably, this low immunogenicity was maintained even under proinflammatory conditions, supporting their suitability for allogeneic application with minimized risk of host immune rejection. Moreover, they lacked alloreactive potential in GvH assays and did not trigger GvHD symptoms in NSG mice, unlike MCAR-T cells which caused lethal toxicity (*SI Appendix,* Fig. S5 *F–K*). These findings confirm that ^{Allo15}MCAR-NKT cells are hypoimmunogenic and non-alloreactive, with a favorable safety profile for off-the-shelf application. Nevertheless, we acknowledge that immunogenicity cannot be fully reflected in studies conducted with immunocompromised mice. Future work will therefore focus on evaluating the immunogenicity of ^{Allo15}MCAR-NKT cells in more physiologically relevant preclinical models, such as humanized mouse models or immunocompetent systems, to better assess potential immune responses in a clinical context (41).

Altogether, our findings establish ^{Allo15}MCAR-NKT cells as a potent, safe, and scalable immunotherapy for PC. The superior cytotoxicity, enhanced tumor homing and infiltration, ability to overcome antigen heterogeneity and escape, and low immunogenicity underscore the translational potential of ^{Allo15}MCAR-NKT cells as an off-the-shelf, allogeneic therapy capable of addressing critical challenges in the treatment of both primary and metastatic PC, and potentially other hard-to-treat solid tumors.

Methods

Mice. NOD.Cg-Prkdc^{SCID}Il2rg^{tm1Wjl}/SzJ (NOD/SCID/IL-2Rγ$^{-/-}$, NSG) mice were maintained in animal facilities of the UCLA. 6- to 10-wk-old mice were used for all experiments. All animal experiments were approved by the Institutional Animal Care and Use Committee (IACUC) of UCLA, and all animal procedures were conducted in accordance with the animal care and use regulations of the Division of Laboratory Animal Medicine at UCLA.

Cell Lines. Human MM cell line MM.1S, chronic myelogenous leukemia cell line K562, PC cell lines ASPC1 and Capan2 were purchased from the ATCC. The parental tumor cell lines were transduced with lentiviral vectors encoding the intended gene(s) to produce stable tumor cell lines overexpressing FG or human MSLN. 72 h post lentivector transduction, cells were subjected to flow cytometry sorting to isolate gene-engineered cells for generating stable cell lines. five stable tumor cell lines were generated for this study, including MM-FG, MM-MSLN-FG, ASPC1-FG, Capan2-FG, and Capan2-MSLN-FG cell lines. The artificial antigen-presenting cell line (aAPC) was generated by engineering the K562 human chronic myelogenous leukemia cell line to overexpress human CD80/CD83/CD86/4-1BBL costimulatory receptors (24). The aAPC-MSLN cell lines were generated by further engineering the parental aAPC line to overexpress human MSLN.

Human CB CD34$^+$ HSPCs and Periphery Blood Mononuclear Cells (PBMCs). Purified CB-derived human CD34$^+$ HSPCs were purchased from HemaCare. Healthy donor PBMCs were provided by the UCLA/CFAR Virology Core Laboratory without identification information under federal and state regulations.

Flow Cytometry. Details of the antibodies, including clone, fluorophore conjugation, and dilution, are provided in the *SI Appendix,* Methods. All flow cytometry staining was performed following standard protocols, as well as specific instructions provided by the manufacturer of a particular antibody. Stained cells were analyzed using a MACSQuant Analyzer 10 flow cytometer (Miltenyi Biotech), following the manufacturers' instructions. FlowJo software version 9 (BD Biosciences) was used for data analysis. For intracellular cytokine staining, the cell products (^{Allo15}MCAR-NKT cells, MCAR-T cells, or quiescent healthy donor–derived T cells) were thawed and resuspended in C10 medium. Cells were stimulated with PMA (Calbiochem, cat. no. 524400; 50 ng/mL) and ionomycin (Calbiochem, cat. no. 407952.; 500 ng/mL) and incubated at 37 °C for 2 h. GolgiStop (BD Biosciences, car. No. 554724; 1.5 μL/mL) was then added to inhibit cytokine secretion, followed by an additional 4-h incubation. Subsequently, intracellular staining was performed using the Cell Fixation/Permeabilization Kit (BD Biosciences, cat. no. 554714) according to the manufacturer's instructions.

Enzyme-Linked Immunosorbent Cytokine Assays (ELISAs). The ELISAs for detecting human cytokines were performed following a standard protocol from BD Biosciences. Supernatants from cell culture assays were collected and assayed to quantify human IFN-γ. The capture and biotinylated pairs for detecting cytokines were purchased from BD Biosciences. The streptavidin–HRP conjugate was purchased from Invitrogen. Human cytokine standards were purchased from eBioscience. Tetramethylbenzidine substrate was purchased from KPL. The samples were analyzed for absorbance at 450 nm using an Infinite M1000 microplate reader (Tecan).

Generation of HSPC-Derived Allogeneic IL-15-Enhanced MCAR-Engineered NKT (^{Allo15}MCAR-NKT) Cells. ^{Allo15}MCAR-NKT cells were generated from gene-engineered human CB CD34$^+$ HSPCs using a 5-stage clinically guided culture method, including HSPC engineering, HSPC expansion, NKT differentiation, NKT deep differentiation, and NKT expansion (24). The detailed protocols have been described previously (28, 71); here we provide a summary of the essential steps in the *SI Appendix, Methods*.

Generation of PBMC-Derived Conventional T Cells. Healthy donor PBMCs were used to generate the PBMC-derived conventional T cells. PBMCs were stimulated with the Dynabeads™ Human T-Activator CD3/CD28 (ThermoFisher Scientific) according to the manufacturer's instructions, followed by culturing in the C10 medium supplemented with human IL-2 (20 ng/mL) for 2 to 3 wk.

Generation of MSLN-Targeting CAR-Engineered Conventional αβ T (MCAR-T) cells. Nontreated tissue culture 24-well or 12-well plates (Corning) were coated with Ultra-LEAF™ Purified Anti-Human CD3 Antibody (Clone OKT3; BioLegend) at 1 μg/mL (500 μL/well), at room temperature for 2 h or alternatively, overnight at

4 °C. Healthy donor PBMCs were resuspended in the C10 medium supplemented with 1 μg/mL Ultra-LEAF™ Purified Anti-Human CD28 Antibody (Clone CD28.2, BioLegend) and 30 ng/mL IL-2, followed by seeding in the precoated plates at 1 × 10^6 cells/mL (1 ml/well). On day 2, cells were transduced with Lenti/MCAR virus for 24 h. The resulting MCAR-T cells were expanded for about 2 wk in C10 medium supplemented with human IL-2, and cryopreserved for future use, following established protocols (24, 25). For all subsequent experiments, conventional MCAR-T cells were either normalized based on the percentage of CAR^+ cells or presorted for CAR expression prior to in vitro and in vivo assays.

Generation of PBMC-Derived IL-15-Enhanced MCAR-Engineered NK (^{PBMC15}MCAR-NK) Cells. Healthy donor PBMCs were sorted with MACS via a Human NK Cell Isolation Kit (Miltenyi Biotech) to enrich NK cells, following the manufacturer's instructions. The enriched NK cells were mixed with irradiated aAPCs at a ratio of 1:10, followed by culturing in C10 medium supplemented with 10 ng/mL IL-7 and IL-15. On day 3, NK cells were transduced with Lenti/MCAR-IL15 viruses for 24 h. The resulting ^{PBMC15}MCAR-NK cells were expanded for about 1 wk in C10 medium supplemented with 10 ng/mL IL-7 and IL-15.

In Vitro Tumor Cell Killing Assay. Tumor cells (1 × 10^4 cells per well) were cocultured with effector cells (at ratios indicated in the figure legends) in Corning 96-well clear bottom black plates for 24 h, in C10 medium with or without the addition of αGC (100 ng/mL). D-luciferin (150 mg/mL, Caliper Life Science) was added to cell cultures to quantify live tumor cells and luciferase activities were read out using an Infinite M1000 microplate reader (Tecan). In experiments that study the NKR-mediated tumor cell killing mechanism, 10 mg/mL LEAF purified anti-human NKG2D (clone 1D11, BioLegend), anti-human DNAM-1 antibody (clone 11A8, BioLegend), or LEAF purified mouse IgG2bk isotype control antibody (clone MG2B-57, BioLegend) was added to cocultures.

In Vitro Serial Tumor Cell Killing Assay. A total of 1 × 10^4 nonengineered tumor cells (e.g., ASPC1 cells; referred to as stimulator cells) was cocultured with 2 × 10^5 effector cells in a Corning 96-well clear bottom black plate in C10 medium. Cultures were supplemented with a dose of 1 × 10^4 stimulator cells every 2 d. 24 h prior to luminescent tumor killing readout, stimulator cells were substituted with 1 × 10^4 of FG-engineered tumor cells (e.g., ASPC1-FG cells; referred to as indicator cells). To quantify the remaining live indicator cells, 100 ml of D-luciferin (10 mg/mL) was added to cell cultures on the day of imaging and the luciferase activities were measured through readout with an Infinite M1000 microplate reader (Tecan).

In Vitro MLR Assay: Studying GvH Response. PBMCs from random healthy donors were irradiated at 2,500 rads and used as stimulators to investigate the GvH response of ^{Allo15}MCAR-NKT cells as responders. Conventional MCAR-T cells were included as a responder control. Stimulators (5 × 10^5 cells/well) and responders (2 × 10^4 cells/well) were cocultured in 96-well round-bottom plates in C10 medium for 4 d; the cell culture supernatants were then collected to measure IFN-γ production using ELISA. Note that the IFN-γ production was solely attributed to ^{Allo15}MCAR-NKT or MCAR-T responder cells.

In Vitro MLR Assay: Studying T Cell–Mediated Allorejection. PBMCs of multiple healthy donors were used as responders, to study the T cell–mediated allorejection of ^{Allo15}MCAR-NKT cells as stimulators (irradiated at 2,500 rads). MCAR-T cells were included as stimulator controls. Stimulators (5 × 10^5 cells/well) and responders (2 × 10^4 cells/well) were cocultured in 96-well round bottom plates in C10 medium for 4 d; the cell culture supernatants were then collected to measure IFN-γ production using ELISA. Note that the IFN-γ production was solely attributed to PBMC responder cells.

In Vivo Bioluminescence Imaging (BLI). BLI was performed using a Spectral Advanced Molecular Imaging HTX system (Spectral Instrument Imaging). Live animal images were captured 5 min after intraperitoneal (i.p.) injection of D-Luciferin to obtain total body bioluminescence. For tissue imaging, mice were i.p. injected with 10 mg of D-Luciferin and killed 5 min postinjection. Subsequently, major organs were harvested and subjected to BLI. The imaging data were analyzed using AURA imaging software (version 3.2.0, Spectral Instrument Imaging). All procedures for the in vivo antitumor efficacy studies using human PC xenograft models are described in the *SI Appendix*, *Methods*.

In Vivo GvHD Evaluation Study of ^{Allo15}MCAR-NKT Cells. On Day 0, NSG mice received i.v. injection of ^{Allo15}MCAR-NKT cells (10 × 10^6 CAR^+ cells in 100 μL PBS per mouse), or MCAR-T cells (10 × 10^6 CAR^+ cells in 100 μL PBS per mouse). Over the experiment, mice were monitored for survival and their body weight and GvHD score were measured. A score ranging from 0 to 2 was assigned for each clinical GvHD sign, which includes body weight, activity, posture, skin thickening, diarrhea, and dishevelment (72). At the end of the experiment, multiple tissues were collected and prepared for histological analysis.

In Vivo CRS Evaluation Study of ^{Allo15}MCAR-NKT Cells. On Day 0, NSG mice received intraperitoneal (i.p.) inoculation of ASPC1-FG cells (5 × 106 cells per mouse). On Day 10, the experimental mice received i.p. injection of vehicle (100 μL PBS per mouse), ^{Allo15}MCAR-NKT cells (10 × 10^6 CAR^+ cells in 100 μL PBS per mouse), or MCAR-T cells (10 x 10^6 CAR^+ cells in 100 μL PBS per mouse). On Days 13, blood samples were collected from the experimental mice, and their serum cytokines (i.e., mouse IL-6, human IFN-γ, TNF-α, IL-2, and IL-6) and mouse SAA-3 were measured using ELISA. A Mouse SAA-3 ELISA Kit (Millipore Sigma) was used to measure SAA-3, following the manufacturer's instructions. Mouse body weight was measured daily from Day 10 to Day 18.

Histology Analysis. Tissues (i.e., pancreases) were harvested from experimental mice, fixed in 10% neutral buffered formalin for up to 36 h, and embedded in paraffin for sectioning (5 mm thickness). Tissue sections were subsequently prepared and stained with anti-GFP or anti-human CD3 by the UCLA Translational Pathology Core Laboratory (TPCL) in accordance with the Core's standard protocols. Stained sections were imaged using an Olympus BX51 upright microscope equipped with an Optronics Macrofire CCD camera (AU Optronics), and the images were analyzed using an Optronics PictureFrame software (AU Optronics).

Statistics. Statistical data analysis was performed using GraphPad Prism 8 software (GraphPad). Student's two-tailed t test was employed for pairwise comparisons. Ordinary one- or two-way ANOVA followed by Tukey's or Dunnett's multiple comparisons test was used for multiple comparisons. Log rank (Mantel–Cox) test adjusted for multiple comparisons was used for Meier survival curves analysis. Data are expressed as the mean ±SEM, unless otherwise indicated. In all figures and figure legends, n denotes the number of samples or animals utilized in the indicated experiments. A p-value of less than 0.05 was considered significant; ns indicates not significant; $*P < 0.05$, $**P < 0.01$, $***P < 0.001$, $****P < 0.0001$.

Data, Materials, and Software Availability. All study data are included in the article and/or *SI Appendix*.

ACKNOWLEDGMENTS. We thank the UCLA animal facility for providing animal support; the UCLA Translational Pathology Core Laboratory (TPCL) for providing histology support; the UCLA CFAR Virology Core for providing human cells. This work was supported by a Partnering Opportunity for Discovery Stage Research Projects Award and a Partnering Opportunity for Translational Research Projects Awards from the California Institute for Regenerative Medicine (DISC2-11157, DISC2-13015, TRAN1-12250, and TRAN1-16050 to L.Y.), a Department of Defense CDMRP PRCRP Impact Award (CA200456 to L.Y.), a Department of Defense Kidney Cancer Research Program Award (KC230215 to L.Y.), a UCLA BSCRC Innovation Award (to L.Y.), and an Ablon Scholars Award (to L.Y.). L.Y. is a member of UCLA Parker Institute for Cancer Immunotherapy (PICI). Y.-R.L. is a postdoctoral fellow supported by a UCLA MIMG M. John Pickett Post-Doctoral Fellow Award, a CIRM-BSCRC Postdoctoral Fellowship, a UCLA Sydney Finegold Postdoctoral Award, a UCLA Chancellor's Award for Postdoctoral Research, and a UCLA Goodman-Luskin Microbiome Center Collaborative Research Fellowship Award.

Author affiliations: [a]Department of Microbiology, Immunology & Molecular Genetics, University of California, Los Angeles, CA 90095; [b]Department of Bioengineering, University of California, Los Angeles, CA 90095; [c]Department of Molecular and Medical Pharmacology, University of California, Los Angeles, CA 90095; [d]Ahmanson Translational Imaging Division, University of California, Los Angeles, CA 90095; [e]Jonsson Comprehensive Cancer Centre, University of California, Los Angeles, CA 90095; [f]Eli and Edythe Broad Centre of Regenerative Medicine and Stem Cell Research, University of California, Los Angeles, CA 90095; [g]Molecular Biology Institute, University of California, Los Angeles, CA 90095; [h]Parker Institute for Cancer Immunotherapy, University of California, Los Angeles, CA 90095; and [i]Goodman-Luskin Microbiome Center, University of California, Los Angeles, CA 90095

1. R. L. Siegel, T. B. Kratzer, A. N. Giaquinto, H. Sung, A. Jemal, Cancer statistics, 2025. *CA Cancer J. Clin.* **75**, 10–45 (2025).
2. J. Kleeff *et al.*, Pancreatic cancer. *Nat. Rev. Dis. Prim.* **2**, 16022 (2016).
3. T. F. Stoop *et al.*, Pancreatic cancer. *Lancet (London, England)* **405**, 1182–1202 (2025).
4. A. Czaplicka, M. Lachota, L. Pączek, R. Zagożdżon, B. Kaleta, Chimeric antigen receptor T cell therapy for pancreatic cancer: A review of current evidence. *Cells* **13**, 101 (2024).
5. C. J. DeSelm, Z. E. Tano, A. M. Varghese, P. S. Adusumilli, CAR T-cell therapy for pancreatic cancer. *J. Surg. Oncol.* **116**, 63–74 (2017).
6. M. A. Aboalela *et al.*, Enhancing mesothelin CAR T cell therapy for pancreatic cancer with an oncolytic herpes virus boosting CAR target antigen expression. *Cancer Immunol. Immunother.* **74**, 202 (2025).
7. X. F. Liu *et al.*, Tumor resistance to anti-mesothelin CAR-T cells caused by binding to shed mesothelin is overcome by targeting a juxtamembrane epitope. *Proc. Natl. Acad. Sci. U.S.A.* **121**, e2317283121 (2024).
8. X. Zhai, L. Mao, M. Wu, J. Liu, S. Yu, Challenges of anti-mesothelin CAR-T-cell therapy. *Cancers (Basel)* **15**, 1357 (2023).
9. R. Hassan *et al.*, Mesothelin-targeting T cell receptor fusion construct cell therapy in refractory solid tumors: Phase 1/2 trial interim results. *Nat. Med.* **29**, 2099–2109 (2023).
10. A. N. Courtney, G. Tian, L. S. Metelitsa, Natural killer T cells and other innate-like T lymphocytes as emerging platforms for allogeneic cancer cell therapy. *Blood* **141**, 869–876 (2023).
11. A. Bendelac, P. B. Savage, L. Teyton, The biology of NKT cells. *Annu. Rev. Immunol.* **25**, 297–336 (2007).
12. M. Kronenberg, Toward an understanding of NKT cell biology: Progress and paradoxes. *Annu. Rev. Immunol.* **23**, 877–900 (2005).
13. E. A. Bae, H. Seo, I. K. Kim, I. Jeon, C. Y. Kang, Roles of NKT cells in cancer immunotherapy. *Arch. Pharm. Res.* **42**, 543–548 (2019).
14. Y.-R. Li *et al.*, Advancing cell-based cancer immunotherapy through stem cell engineering. *Cell Stem Cell* **30**, 592–610 (2023), 10.1016/j.stem.2023.02.009.
15. Y.-R. Li, Y. Zhu, Y. Chen, L. Yang, The clinical landscape of CAR-engineered unconventional T cells. *Trends Cancer* **11**, 520–539 (2025), 10.1016/j.trecan.2025.03.001.
16. D. Bollino, T. J. Webb, Chimeric antigen receptor-engineered natural killer and natural killer T cells for cancer immunotherapy. *Transl. Res.* **187**, 32–43 (2017).
17. A. Rotolo *et al.*, Enhanced anti-lymphoma activity of CAR19-iNKT cells underpinned by dual CD19 and CD1d targeting. *Cancer Cell* **34**, 596–610.e11 (2018).
18. A. Heczey *et al.*, Anti-GD2 CAR-NKT cells in relapsed or refractory neuroblastoma: Updated phase 1 trial interim results. *Nat. Med.* **29**, 1379–1388 (2023), 10.1038/s41591-023-02363-y.
19. A. Heczey *et al.*, Anti-GD2 CAR-NKT cells in patients with relapsed or refractory neuroblastoma: An interim analysis. *Nat. Med.* **26**, 1686–1690 (2020).
20. Y.-R. Li *et al.*, Allogeneic CD33-directed CAR-NKT cells for the treatment of bone marrow-resident myeloid malignancies. *Nat. Commun.* **16**, 1248 (2025).
21. Y.-R. Li, K. Zhou, Y. Zhu, T. Halladay, L. Yang, Breaking the mold: Unconventional T cells in cancer therapy. *Cancer Cell* **43**, 317–322 (2024), 10.1016/j.ccell.2024.11.010.
22. Y. Chen, Y. Zhu, Y.-R. Li, in *The Role of Innate T Cells in Cancer BT - Handbook of Cancer and Immunology*, N. Rezaei, Ed. (Springer International Publishing, 2022), pp. 1–18.
23. Y. R. Li *et al.*, Development of off - the - shelf hematopoietic stem cell–engineered invariant natural killer T cells for COVID-19 therapeutic intervention. *Stem Cell Res. Ther.* **13**, 112 (2022), 10.1186/s13287-022-02787-2.
24. Y.-R. Li *et al.*, Generation of allogeneic CAR-NKT cells from hematopoietic stem and progenitor cells using a clinically guided culture method. *Nat. Biotechnol.* **43**, 329–344 (2024), 10.1038/s41587-024-02226-y.
25. Y.-R. Li *et al.*, Development of allogeneic HSC-engineered iNKT cells for off-the-shelf cancer immunotherapy. *Cell Rep. Med.* **2**, 100449 (2021).
26. A. R. Haas *et al.*, Phase I study of lentiviral-transduced chimeric antigen receptor-modified T cells recognizing mesothelin in advanced solid cancers. *Mol. Ther.* **27**, 1919–1929 (2019).
27. C. A. Ramos *et al.*, In vivo fate and activity of second- versus third-generation CD19-specific CAR-T cells in B cell non-Hodgkin's lymphomas. *Mol. Ther.* **26**, 2727–2737 (2018).
28. Y.-R. Li *et al.*, Generating allogeneic CAR-NKT cells for off-the-shelf cancer immunotherapy with genetically engineered HSP cells and feeder-free differentiation culture. *Nat. Protoc.* **20**, 1352–1388 (2025), 10.1038/s41596-024-01077-w.
29. E. Liu *et al.*, GMP-compliant universal antigen presenting CELLS (uAPC) promote the metabolic fitness and antitumor activity of armored cord blood CAR-NK cells. *Front. Immunol.* **12**, 626098 (2021).
30. E. Y. Kim, L. Lynch, P. J. Brennan, N. R. Cohen, M. B. Brenner, The transcriptional programs of *i*NKT cells. *Semin. Immunol.* **27**, 26–32 (2015).
31. J. Liu *et al.*, The peripheral differentiation of human natural killer T cells. *Immunol. Cell Biol.* **97**, 586–596 (2019).
32. D. I. Godfrey, J. Le Nours, D. M. Andrews, A. P. Uldrich, J. Rossjohn, Unconventional t cell targets for cancer immunotherapy. *Immunity* **48**, 453–473 (2018).
33. C. S. Seet *et al.*, Generation of mature T cells from human hematopoietic stem and progenitor cells in artificial thymic organoids. *Nat. Methods* **14**, 521–530 (2017).
34. R. N. Germain, T-cell development and the CD4–CD8 lineage decision. *Nat. Rev. Immunol.* **2**, 309–322 (2002).
35. R. Benjamin *et al.*, Preliminary data on safety, cellular kinetics and anti-leukemic activity of UCART19, an allogeneic anti-CD19 CAR T-cell product, in a pool of adult and pediatric patients with high-risk CD19+ relapsed/refractory B-cell acute lymphoblastic leukemia. *Blood* **132**, 896–896 (2018).
36. L. A. Murphy *et al.*, Digital polymerase chain reaction strategies for accurate and precise detection of vector copy number in chimeric antigen receptor T-cell products. *Cytotherapy* **25**, 94–102 (2023).
37. J. Chen *et al.*, Anti-mesothelin CAR-T immunotherapy in patients with ovarian cancer. *Cancer Immunol. Immunother.* **72**, 409–425 (2023).
38. E. Schoutrop *et al.*, Mesothelin-specific CAR t cells target ovarian cancer. *Cancer Res.* **81**, 3022–3035 (2021).
39. A. R. Haas *et al.*, Two cases of severe pulmonary toxicity from highly active mesothelin-directed CAR T cells. *Mol. Ther.* **31**, 2309–2325 (2023).
40. A. Klampatsa, V. Dimou, S. M. Albelda, Mesothelin-targeted CAR-T cell therapy for solid tumors. *Expert Opin. Biol. Ther.* **21**, 473–486 (2021).
41. Y.-R. Li *et al.*, Managing allorejection in off-the-shelf CAR-engineered cell therapies. *Mol. Ther.* **33**, 2368–2390 (2024), 10.1016/j.ymthe.2024.11.035.
42. Y. Chen *et al.*, Genetic engineering strategies to enhance antitumor reactivity and reduce alloreactivity for allogeneic cell-based cancer therapy. *Front. Med.* **10**, 1135468 (2023).
43. Y.-R. Li *et al.*, Engineering allorejection-resistant CAR-NKT cells from hematopoietic stem cells for off-the-shelf cancer immunotherapy. *Mol. Ther.* **32**, 1849–1874 (2024), 10.1016/j.ymthe.2024.04.005.
44. S. Depil, P. Duchateau, S. A. Grupp, G. Mufti, L. Poirot, "Off-the-shelf" allogeneic CAR T cells: Development and challenges. *Nat. Rev. Drug Discov.* **19**, 185–199 (2020).
45. J. A. Marin-Acevedo *et al.*, Next generation of immune checkpoint therapy in cancer: New developments and challenges. *J. Hematol. Oncol.* **11**, 39 (2018).
46. A. C. Anderson, N. Joller, V. K. Kuchroo, Lag-3, Tim-3, and TIGIT: Co-inhibitory receptors with specialized functions in immune regulation. *Immunity* **44**, 989–1004 (2016).
47. C. Sun, G. Dotti, B. Savoldo, Utilizing cell-based therapeutics to overcome immune evasion in hematologic malignancies. *Blood* **127**, 3350–3359 (2016).
48. Y.-R. Li, T. Halladay, L. Yang, Immune evasion in cell-based immunotherapy: Unraveling challenges and novel strategies. *J. Biomed. Sci.* **31**, 5 (2024).
49. W. Qiu, G. H. Su, Development of orthotopic pancreatic tumor mouse models. *Methods Mol. Biol.* **980**, 215–223 (2013).
50. N. Nagarsheth, M. S. Wicha, W. Zou, Chemokines in the cancer microenvironment and their relevance in cancer immunotherapy. *Nat. Rev. Immunol.* **17**, 559–572 (2017).
51. G. H. Ran *et al.*, Natural killer cell homing and trafficking in tissues and tumors: From biology to application. *Signal Transduct. Target. Ther.* **7**, 205 (2022).
52. D. Slauenwhite, B. Johnston, Regulation of NKT cell localization in homeostasis and infection. *Front. Immunol.* **6**, 255 (2015).
53. S. Y. Thomas *et al.*, CD1d-restricted NKT cells express a chemokine receptor profile indicative of Th1-type inflammatory homing cells. *J. Immunol.* **171**, 2571–2580 (2003).
54. C. H. Kim, B. Johnston, E. C. Butcher, Trafficking machinery of NKT cells: Shared and differential chemokine receptor expression among Vα24+Vβ11+ NKT cell subsets with distinct cytokine-producing capacity. *Blood* **100**, 11–16 (2002).
55. F. Alrumaihi, The multi-functional roles of CCR7 in human immunology and as a promising therapeutic target for cancer therapeutics. *Front. Mol. Biosci.* **9**, 834149 (2022).
56. A. Shiner, R. C. Sperandio, M. Naimi, U. Emmenegger, Prostate cancer liver metastasis: An ominous metastatic site in need of distinct management strategies. *J. Clin. Med.* **13**, 734 (2024).
57. C. J. Halbrook, C. A. Lyssiotis, M. Pasca di Magliano, A. Maitra, Pancreatic cancer: Advances and challenges. *Cell* **186**, 1729–1754 (2023).
58. N. J. Hess, M. E. Brown, C. M. Capitini, G. V. H. D. Pathogenesis, Prevention and treatment: Lessons from humanized mouse transplant models. *Front. Immunol.* **12**, 723544 (2021).
59. Y.-R. Li, Y. Zhu, Y. Fang, Z. Lyu, L. Yang, Emerging trends in clinical allogeneic CAR cell therapy. *Med. (New York, N.Y.)* **6**, 100677 (2025), 10.1016/j.medj.2025.100677.
60. Z. Lyu *et al.*, Addressing graft-versus-host disease in allogeneic cell-based immunotherapy for cancer. *Exp. Hematol. Oncol.* **14**, 66 (2025).
61. A. B. Pillai, T. I. George, S. Dutt, P. Teo, S. Strober, Host NKT cells can prevent graft-versus-host disease and permit graft antitumor activity after bone marrow transplantation. *J. Immunol.* **178**, 6242–6251 (2007).
62. T. Coman *et al.*, Human CD4-invariant NKT lymphocytes regulate graft versus host disease. *Oncoimmunology* **7**, 1–10 (2018).
63. S. S. Neelapu *et al.*, Chimeric antigen receptor t-cell therapy - Assessment and management of toxicities. *Nat. Rev. Clin. Oncol.* **15**, 47–62 (2018).
64. J. N. Brudno, J. N. Kochenderfer, Toxicities of chimeric antigen receptor T cells: Recognition and management. *Blood* **127**, 3321–3330 (2016).
65. T. Giavridis *et al.*, CAR T cell-induced cytokine release syndrome is mediated by macrophages and abated by IL-1 blockade letter. *Nat. Med.* **24**, 731–738 (2018).
66. W. J. Ho, E. M. Jaffee, L. Zheng, The tumour microenvironment in pancreatic cancer – Clinical challenges and opportunities. *Nat. Rev. Clin. Oncol.* **17**, 527–540 (2020).
67. A.-L. Xia, X.-C. Wang, Y.-J. Lu, X.-J. Lu, B. Sun, Chimeric-antigen receptor T (CAR-T) cell therapy for solid tumors: Challenges and opportunities. *Oncotarget* **8**, 90521–90531 (2017).
68. L. A. Kankeu Fonkoua, O. Sirpilla, R. Sakemura, E. L. Siegler, S. S. Kenderian, CAR T cell therapy and the tumor microenvironment: Current challenges and opportunities. *Mol. Ther. Oncol.* **25**, 69–77 (2022).
69. X. Chen, F. Liu, Q. Xue, X. Weng, F. Xu, Metastatic pancreatic cancer: Mechanisms and detection (review). *Oncol. Rep.* **46**, 231 (2021).
70. K. Watanabe *et al.*, Pancreatic cancer therapy with combined mesothelin-redirected chimeric antigen receptor T cells and cytokine-armed oncolytic adenoviruses. *JCI Insight* **3**, e99573 (2018).
71. Y.-R. Li *et al.*, Overcoming ovarian cancer resistance and evasion to CAR-T cell therapy by harnessing allogeneic CAR-NKT cells. *Med. (New York, N.Y.)* **6**, 100804 (2025), 10.1016/j.medj.2025.100804.
72. Y.-R. Li *et al.*, Off-the-shelf third-party HSC-engineered iNKT cells for ameliorating GvHD while preserving GvL effect in the treatment of blood cancers. *iScience* **25**, 104859 (2022).